Bulk Acoustic Resonator Devices using ZnO-Based Film and Back Cavity

Xin Li, Mengwei Liu, and Yanlu Feng

Abstract**—**The purpose of this study was to investigate bulk acoustic resonator (FBAR) devices using ZnO-based film and back cavity. A Mason equivalent circuit model was adopted to simulate the impedance characteristics of FBAR devices. The influence of piezoelectric material thickness, electrode thickness, and resonance area on the impedance characteristics of FBAR devices was analyzed. Structural parameters of the FBAR devices were designed, and bulk silicon micromachining was applied to fabricate Al/ZnO/Al-based FBAR devices with a back cavity. X-ray diffraction analysis shows that ZnO piezoelectric films have a highly preferred c-axis orientation. The frequency response of longitudinal wave FBAR devices has been measured by an RF network analyzer, and the results indicate the series resonant frequency and parallel resonant frequency of the fabricated FBAR devices determined to be 1.546 GHz and 1.590 GHz, respectively, which are close to the simulated results. According to the measured results, the effective electromechanical coupling coefficient and the quality factor have been calculated to be 6.83% and 350, respectively. The findings of this study may serve as reference for the development of FBAR devices.

Keywords**—**back cavity, bulk silicon micromachining, film bulk acoustic resonator, ZnO piezoelectric film

I. INTRODUCTION

The wireless communication technology has developed rapidly in recent years. Frequencies have increased from 500 MHz to 6 GHz, and the device circuitry has become progressively miniaturized and integrated. As important elements in RF circuits, filters have also had to shrink and integrate. Common surface acoustic wave filters and dielectric ceramic filters in common use no longer meet these requirements. The appearance of thin film acoustic resonator (FBAR) devices has led to their development [1–3]. Featuring high-frequency support, high Q, greater power capacity, and compatibility with CMOS-integrated circuit technology [4-5], FBARs are important devices among next generation filters [6-7].

Design and fabrication of FBAR devices have attracted the attention of manufacturers as design and manufacturing technology for the FBAR devices needs additional research. In this paper, we explore several facets of FBAR design. We have simulated the impedance characteristics of FBAR devices using the Mason equivalent circuit model and have analyzed the influence of piezoelectric material thickness, electrode thickness, and resonance area on those characteristics. We have also established structural parameters of some FBAR devices and fabricated Al/ZnO/Al-based FBAR devices with a back cavity using bulk silicon micromachining. We then measured and analyzed our devices.

II. FBAR DEVICES

A. *Working principle*

Body longitudinal acoustic waves and body shear acoustic waves can be excited in piezoelectric material. When acoustic waves propagate along the c-axis direction in the piezoelectric material, if the displacement direction of the acoustic wave particle is parallel to the wave propagation direction, the excited bulk acoustic waves are longitudinal. When the displacement direction of the acoustic wave particle is perpendicular to the wave propagation direction, the excited bulk acoustic waves are shear [8]. Our FBAR device vibrates along the thickness direction with vibration belonging to the longitudinal wave mode [9]. Thus, we neglect the influence of shear waves.

An ideal FBAR device is composed of a lower electrode, the piezoelectric film, and an upper electrode, as shown in Fig. 1. When an AC voltage signal $V(f)$ is applied to the upper and lower electrodes of the device, the piezoelectric material between the two electrodes undergoes mechanical deformation due to the inverse piezoelectric effect. With a changing electric field, contraction and expansion of the piezoelectric film leads to vibration. The vibration produces bulk acoustic waves propagating along the thickness direction in the piezoelectric material. When the bulk acoustic waves propagate to the interface between either electrode and the air, they are reflected back. The waves thus bounce back and forth in the piezoelectric material forming oscillations. Thanks to the positive piezoelectric effect of the piezoelectric film, the oscillating acoustic waves produce a radio frequency signal. When the propagation distance of bulk acoustic waves in the piezoelectric film is equal to the half wavelength or an odd multiple of the half wavelength, the standing wave oscillation forms and produces resonance [10].

The electrical impedance characteristics of the FBAR are

This work was supported in part by the National Natural Science Foundation of China under Grant 10804119 and the Liaoning Province Education Office under Grant LFGD2017015.

Xin Li is with School of Information Science and Engineering, Shenyang University of Technology, Shenyang, 110870 China (Tel: 0086-24-25496381; fax: 0086-24-25496349; e-mail: lixin97@163.com).

Mengwei Liu is with Institute of Acoustics, Chinese Academy of Science, Beijing 100190, China (e-mail: liumw@mail.ioa.ac.cn).

Yanlu Feng is with School of Information Science and Engineering, Shenyang University of Technology, Shenyang, 110870 China (e-mail: 1194355789@qq.com).

shown in Fig. 2. The devices have a series resonant frequency f_s and a parallel resonant frequency f_p. When a given AC voltage is applied, the series resonant frequency f_s of the device is obtained under the following conditions: the polarization vector P and the electrical field E are in phase within the piezoelectric film, the generated current is at maximum, and the electrical impedance of the FBAR is at minimum. The parallel resonant frequency f_p is obtained when the polarization vector P and the electrical field E are completely out of phase, the generated current is at minimum, and the electrical impedance of the FBAR is at maximum.

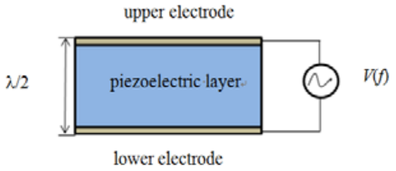

Fig. 1 the structure diagram of an ideal FBAR

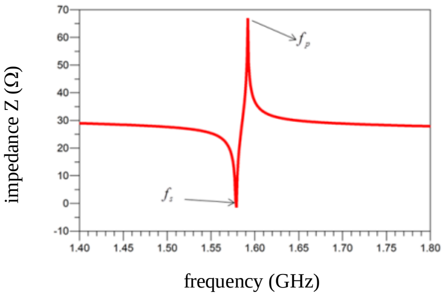

Fig. 2 electrical impedance characteristics of an FBAR

B. *The device parameters*

In addition to f_s and f_p, the effective electromechanical coupling coefficient and the quality factor Q are two important parameters in evaluating the performance of the FBAR devices. These parameters are defined according to the equations [11]

$$K_{eff}{}^2 = \left(\frac{\pi}{2}\right)^2 \frac{f_p - f_s}{f_p} \quad \text{and} \tag{1}$$

$$Q_{f_x} = \frac{f_x}{2}\left|\frac{\mathrm{d}\angle Z_{in}}{\mathrm{d}\,f}\right|_{f_x}, \tag{2}$$

The effective electromechanical coupling coefficient $K_{\text{eff}}{}^2$ represents the conversion degree between the mechanical and electrical energy in the device. The bandwidth of an FBAR filter increases with increasing $K_{\text{eff}}{}^2$. $K_{\text{eff}}{}^2$ depends primarily on the piezoelectric material with a secondary dependency on the thickness of the upper and the lower electrode layers.

The quality factor Q indicates the bulk acoustic wave loss in the FBAR and the insertion loss of the FBAR filter. The in-band insertion loss decreases with increasing Q. Q depends not only on the acoustic wave loss in the electrode and piezoelectric materials but also on the degree of confinement of the bulk acoustic waves within the sandwich structure. The loss of bulk acoustic waves in the material and the degree of leakage in the FBAR decreases with increasing Q. In actual production, the Q value is enhanced primarily by the high-quality manufacture and orientation of the piezoelectric film.

C. *Structure of the FBAR*

According to transmission line theory, the incident wave is reflected back when the load is infinite or zero. Thus, the acoustic impedance of the upper and lower boundary in the sandwich structure must be infinite or zero. Since the acoustic impedance of the air is approximately zero, it serves as the better acoustic limiting interface. Another acoustic limiting interface is a Bragg reflection layer composed of 1/4 wavelength deposition layers with alternating high and low acoustic impedances. The surface of the upper electrode in an FBAR device is usually in contact with the air. However, the lower surface of the FBAR device is usually in contact with a substrate material such as silicon making it necessary to form a better acoustic limited interface via the etching process.

MEMS micromachining etches away most of silicon on the back of the device, forming a back cavity and creating the interface between the air and the metal on the surface of the lower electrode. With air at both electrodes, the generated acoustic waves are confined in the sandwich structure. For silicon substrates, the etching process typically uses wet etching or Inductively Coupled Plasma. Either method removes most of the substrate when forming the FBAR device, yielding a device with poor mechanical strength. The devices are easily broken during production, decreasing the yield. To address this problem, low stress silicon nitride or silicon dioxide is deposited as a support layer below the lower electrode to improve mechanical rigidity at the expense of a reduced Q value [12]. Fig. 3 shows an FBAR device with a back cavity.

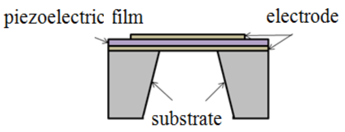

Fig. 3 an FBAR with back cavity

III. DEVICE SIMULATION AND ANALYSIS

A. *Mason equivalent circuit model*

The general analytic expression for the impedance of the piezoelectric layer in an FBAR device is derived from acoustic theory and given in Formula 3[13].

$$Z = \frac{1}{j\omega C_0}\left[1 - k_t^2 \frac{\tan\theta}{\theta} \frac{(z_t + z_b)\cos^2\theta + j\sin 2\theta}{(z_t + z_b)\cos 2\theta + j(z_t z_b + 1)\sin 2\theta}\right] \tag{3}$$

The above formula is properly mathematically processed. The transformed formula is expressed as

$$Z = \frac{1}{j\omega C_0 + \dfrac{1}{-\dfrac{1}{j\omega C_0} + n^2\left(-jZ_P \csc 2\theta + \dfrac{1}{\dfrac{1}{jZ_P \tan\theta + Z_t} + \dfrac{1}{jZ_P \tan\theta + Z_b}}\right)}} \tag{4}$$

where C_0 is the static capacitance; θ is the phase displacement; $k_t{}^2$ is the electromechanical coupling coefficient; and z_t and z_b

are the normalized acoustic impedances at the upper and lower surfaces of the piezoelectric material, respectively. (Regarding the normalized acoustic impedances, $z_t=Z_t/Z_p$ and $z_b=Z_b/Z_p$, where Z_p is the characteristic acoustic impedance of the piezoelectric materials and Z_t and Z_b are the acoustic impedances at the upper and lower surfaces of the piezoelectric material, respectively.) Additionally, $n^2=2\theta/k^2_t\omega C_0 Z_p$ represents the transformer in AC circuits. The usual symbols represent the inductance and the impedance. Therefore, Formula 4 can be represented with a Mason equivalent circuit for the piezoelectric material as shown in Fig. 4, with $Z_d=jZ_P\tan\theta$ and $Z_e=jZ_P\csc 2\theta$. For an ideal FBAR device, $Z_t=Z_b=0$.

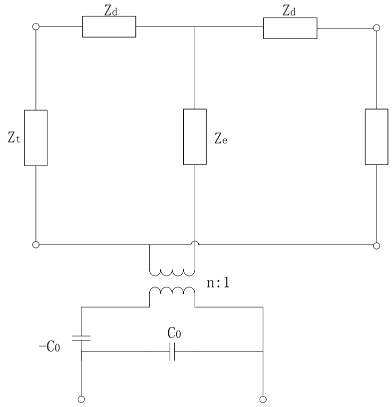

Fig. 4 the Mason equivalent circuit of the piezoelectric layer

In the circuit, $C_0=\varepsilon^S_{zz}A/2d$ and $\theta=\omega d/v_a$, where A represents the effective area of FBAR, ε^S_{zz} represents the clamped dielectric constant, $2d$ represents the thickness of the piezoelectric layer, and v_a represents the longitudinal wave velocity. From these values along with the characteristic acoustic impedance Z_p and the acoustic impedances Z_t and Z_b, we obtain the Mason equivalent circuit of the corresponding piezoelectric layer.

In an FBAR device with a composite structure, the bulk acoustic waves propagate not only along the c-axis in the piezoelectric layer but also in the ordinary acoustic layer, the upper and lower electrode layers, the Bragg reflection layer, and the supporting layer. Therefore, electromagnetic transmission line theory can be adopted to express the transmission of acoustic waves in the ordinary acoustic layer. The transformer in Figure 4 represents the conversion between mechanical energy and electrical energy. Therefore, the Mason equivalent circuit of the ordinary acoustic layer assumes the form shown in Figure 5, where Z_f and Z_g represent the acoustic impedances, Z_{in} represents the input impedance, and Z_L represents the load acoustic impedance.

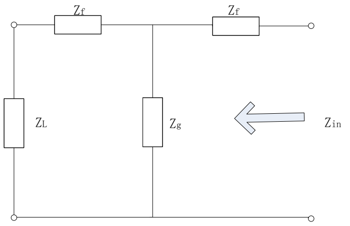

Fig. 5 the Mason equivalent circuit of the ordinary acoustic layer

The expression for Z_{in} obtained from Figure 5 is

$$\begin{aligned} Z_{in} &= Z_f + \frac{(Z_L+Z_f)Z_g}{Z_L+Z_f+Z_g} \qquad (5) \\ &= \frac{Z_L(Z_f+Z_g)+Z_f^2+2Z_fZ_g}{Z_L+Z_f+Z_g} \\ &= Z_0\frac{Z_L+\dfrac{Z_f^2+2Z_fZ_g}{Z_f+Z_g}}{Z_0+Z_L\dfrac{Z_0}{Z_f+Z_g}}, \end{aligned}$$

and from transmission line theory, the expression for Z_{in} is

$$Z_{in}=Z_0\frac{Z_L+jZ_0\tan(kd)}{Z_0+jZ_L\tan(kd)}, \qquad (6)$$

Where Z_0 is the characteristic acoustic impedance, k is the acoustic transmission constant, and d is the thickness of the acoustic layer. Comparing Formulas (5) and formula (6), we obtain the formulas (7) and (8)

$$\frac{Z_f^2+2Z_fZ_g}{Z_f+Z_g}=jZ_0\tan(kd) \qquad (7)$$

$$\frac{Z_0}{Z_f+Z_g}=j\tan(kd)\cdot \qquad (8)$$

Applying trigonometric transformations to Formulas (7) and (8), we obtain

$$Z_f=jZ_0\tan(\frac{kd}{2}) \qquad (9)$$

$$Z_g=\frac{Z_0}{j\sin(kd)}\cdot \qquad (10)$$

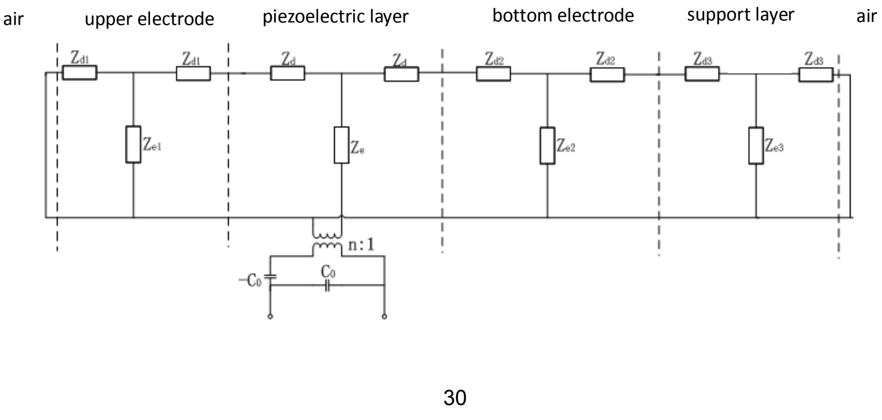

Fig. 6 the Mason equivalent circuit of the FBAR

Fig. 6 shows the Mason equivalent circuit diagram of an FBAR device where f_s and f_p are the series resonant frequency and the parallel resonant frequency of the FBAR devices, respectively; f_x represents either the series resonant frequency or the parallel resonant frequency; and $\angle Z_{in}$ is the impedance phase in radians. The upper and lower electrode, piezoelectric, and supporting layers are cascaded together to obtain the Mason equivalent circuits. We can analyze different cascading forms depending on the requirements in actual simulation.

B. *FBAR simulation*

We used the ADS (Advanced Design System) software from Agilent for our tests [14]. Fig. 7 shows the ADS simulation scheme. The fabricated FBAR has an upper Al electrode layer, a ZnO piezoelectric layer, and an Al lower electrode layer. All layers are 0.1μm thick.

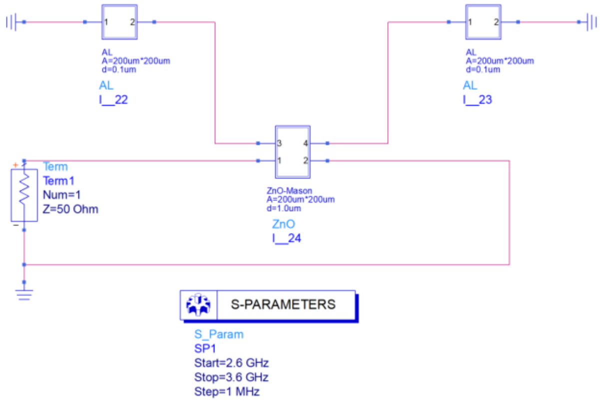

Fig. 7 the ADS simulation of an actual FBAR

The simulation results of the impedance characteristics are shown in Fig. 8. The thick line represents the amplitude frequency characteristic of the FBAR, and the fine line represents the phase frequency characteristic. The figure shows that the theoretical values of the series and parallel resonant frequencies of the FBAR device are 1.579GHz and 1.592GHz, respectively.

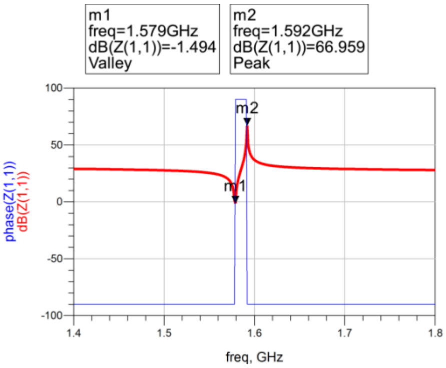

Fig. 8 impedance characteristic of a fabricated FBAR

C. *Analysis of FBAR performance*

1) Influence of the piezoelectric material thickness on the impedance characteristics of an FBAR

The impedance characteristic curves of the FBAR with ZnO thicknesses of 0.7μm, 1μm, 1.3μm and 1.6μm are shown in Figure 9. The upper Al electrode layer thickness, lower Al electrode layer thickness and resonance area are 0.1μm, 1μm, 200μm×200μm, respectively. The resonant frequency of the FBAR gradually decreases with the increase of the ZnO layer thickness.

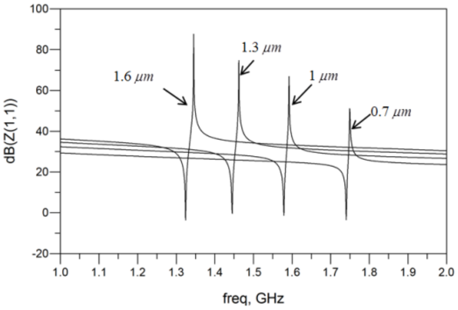

Fig.9 impedance of FBARs with ZnO of different thicknesses

2) Influence of the upper electrode thickness on the impedance characteristics of an FBAR

The impedance characteristic curves of an FBAR with upper Al electrode thicknesses of 0.1μm, 0.13μm, 0.16μm and 0.19μm are shown in Figure 10. The ZnO layer thickness, lower Al electrode layer thickness, and resonance area are 1μm, 1μm, and 200μm×200μm, respectively. Fig.10 shows that the resonant frequency of the FBAR decreases as the thickness of the upper Al electrode increases. The propagation path of the bulk acoustic waves increases with the increase of the electrode thickness, resulting in a decrease in the resonant frequency.

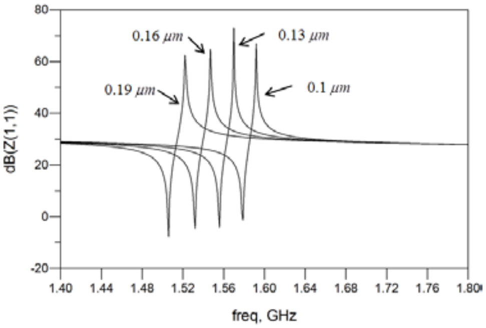

Fig. 10 impedance of FBARs with electrodes of different thicknesses

3) Influence of the resonant area on the impedance characteristics of an FBAR

Fig. 11 shows the impedance characteristic curves of FBAR devices with resonance areas of 200μm×200μm, 300μm×300μm and 400μm×400μm. The thicknesses of the upper Al electrode, ZnO piezoelectric layer, and lower Al electrode layers are all 0.1μm. From Fig. 11, one sees that the resonant frequency is independent of the resonance area. As the resonance area increases, the impedance of the non-resonance region decreases.

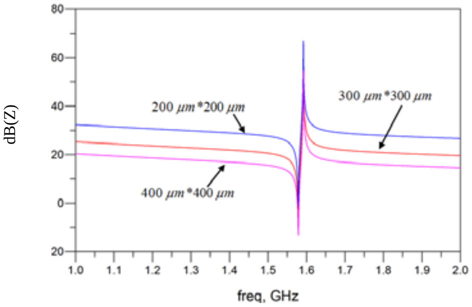

Fig. 11 impedance of FBARs with different resonance areas

The structure of the filter can be optimized using these FBAR performance characteristics.

D. Optimal design of FBAR structure

According to the simulation analysis, the series and parallel resonance frequencies of the FBAR are related to the thickness of the piezoelectric material and electrodes. The ADS software determined the optimal thickness of the piezoelectric material, enabling calculation of the required series and parallel resonant frequencies of the FBAR.

The resonant frequency of our fabricated FBAR device is about 1.5GHz using a ZnO piezoelectric layer thickness of 2μm and upper and lower Al electrode thicknesses of 0.1μm and 1μm, respectively. We left the electrode thickness unchanged and optimized other parameters by changing the thickness of the ZnO piezoelectric layer. Fig. 12 shows the impedance characteristic of an optimized FBAR device. The thickness of ZnO piezoelectric layer after optimization was 1.171μm with a series resonance frequency of 1.5 GHz. The thickness of the upper Al electrode layer, ZnO piezoelectric layer and lower Al electrode layer in the final design of the FBAR device are 0.1μm, 1μm and 1μm, respectively.

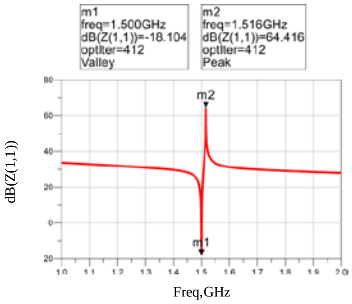

Fig. 12 the optimized impedance characteristic of an FBAR

IV. FABRICATION OF FBAR DEVICES

Fig. 13 shows the manufacturing process for FBAR devices.

a) The silicon wafer is cleaned and dried.

b) An approximately 5000Å silicon nitride thin film is grown on the front side of silicon wafer by Plasma enhanced chemical vapor deposition, with the silicon nitride subsequently annealed to relieve the residual stress.

c) A layer of aluminum is grown on both sides of the silicon wafer using ion beam sputtering, with the positive aluminum layer forming the lower electrode, and the opposite layer used as the masking layer for dry etching.

d) Standard lithography is applied to etch the aluminum to form the lower electrode on the front side of the silicon wafer. The double side alignment process is used to define the etching window for Inductively Coupled Plasma on the back side of the silicon wafer, with concentrated phosphoric acid used to etch away the aluminum film in the window area.

e) The zinc oxide film is deposited on the lower electrode by magnetron sputtering, followed by photolithography.

f) The lift-off process is used to form the upper electrode on the zinc oxide piezoelectric material.

g) The front side of the wafer is protected while Inductively Coupled Plasma etching removes the needed large amount of silicon and silicon nitride from the back until the structure is completely released as the final FBAR device.

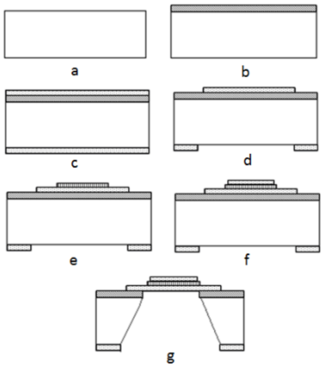

Fig. 13 the manufacturing process of an FBAR

Aluminum and zinc oxide are used for the electrodes and piezoelectric layer, respectively. The use of Inductively Coupled Plasma etching for the back of the device solves the silicon fragility problem. The front and back of an FBAR with a circular electrode is shown in Fig. 14. The small circle in the Fig. 14a is the upper electrode of the FBAR, and the big circle is the lower electrode of the FBAR, The zinc oxide film is sandwiched between them.

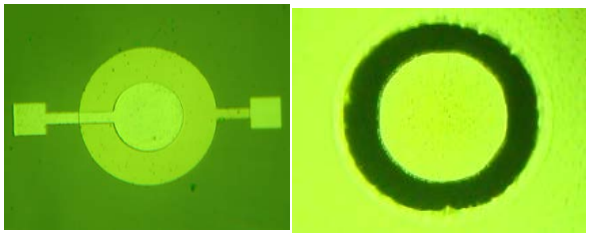

(a) The front of an FBAR (b) The back of an FBAR

Fig. 14 a fabricated FBAR device

V. RESULTS AND ANALYSIS

The ZnO piezoelectric film in the FBAR devices vibrates along the thickness direction to form resonance, ZnO piezoelectric to be oriented along the c-axis. Fig. 15 shows the X-ray Diffraction curve of ZnO film. When 2θ=34.6°, there is an obvious diffraction peak in the film indicating that ZnO piezoelectric films produced by sputtering have a high preference for orientation along the c-axis direction.

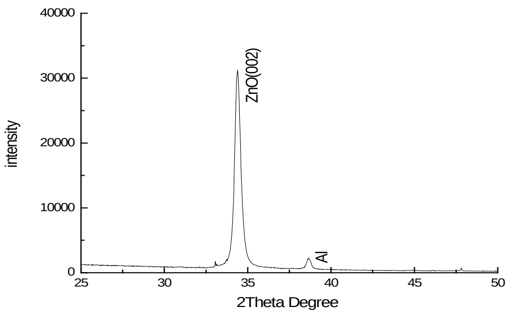

Fig. 15 X-ray diffraction curves of ZnO film

The electrode of our FBAR was welded to the PCB board, and we used an Agilent E5071C RF network analyzer for measurement. The S22 test diagram of the amplitude frequency characteristic is shown in Fig. 16. The resonance characteristics of our fabricated FBAR device are obvious.

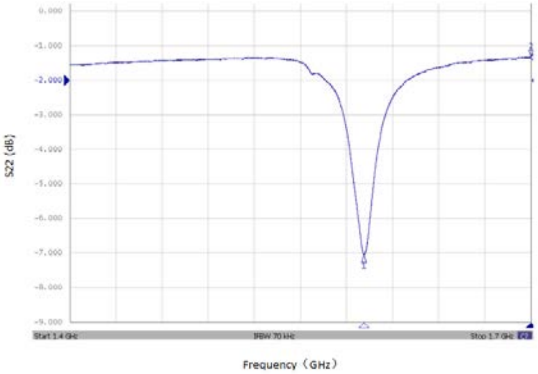

Fig. 16 the S22 measurement results of an FBAR device

The fabricated devices have two resonant frequencies: the series resonant frequency of 1.546 GHz and the parallel resonant frequency of 1.590 GHz, which are similar to the previous theoretical simulation results of 1.579 GHz and 1.592 GHz. According to Formulas (1) and (2) and the experimental data, K_{eff}^2 and Q for our fabricated FBAR devices were calculated to be 6.83% and 350, respectively.

VI. CONCLUSION

We analyzed the influence of the thickness of the ZnO thin film, the thickness of the electrodes, and the effective resonance area of the FBAR device on the impedance characteristics of the device. We also developed a suitable fabrication process for an FBAR device with a back cavity and used an Agilent E5071C RF network analyzer to measure a fabricated FBAR. The series and parallel resonant frequencies were both similar to the theoretical results obtained with software simulation. The good K_{eff}^2 and Q values of the fabricated FBAR devices were expected. The RF filters and duplexers based on the FBAR devices will be used widely in wireless mobile communication systems.

REFERENCES

[1] K. M. Lakin and J. S. Wang, “Acoustic bulk wave composite resonators,” Appl. Phys.Lett, vol. 38, no. 3, pp. 125–127, Mar. 1981.
[2] Sang-Ho Kim, Jae-Sung Lee, Hyun-Chul Choi and Yong-Hyun Lee, “The fabrication of thin-film bulk acoustic wave resonators employing a ZnO/Si composite diaphragm structure using porous silicon layer etching,” IEEE Electron Device Letters, vol. 20, no. 3, pp. 113-115, Mar. 1999.
[3] Y. C. Chen, “Modeling of thin film bulk acoustic wave resonators and ladder-type filter design”, Journal of optoelectronics and advanced materials, vol. 12, no. 9, pp. 1993-1999, Sept 2010.
[4] J. Gao, G.Liu, J. Li, G. Li, “Recent developments of film bulk acoustic resonators,” Functional Materials Letters, Vol. 9, no. 3, pp. 163-173, Mar. 2016.
[5] P. C. Tembhare, P. H. Rangaree, “A review on: design of 2.4GHz FBAR filter using MEMS technology for RF applications,” Imperial Journal of Interdisciplinary Research, vol. 3, no. 3, pp. 939-941, Mar. 2017.
[6] P. Raju, D. Boolchandani, K.J. Rangra, “Design of MEMS based film bulk acoustic wave resonator,” Materials Today: Proceedings, vol. 4, no. 9, pp. 10377–10382, Sept. 2017.
[7] A.J. Flewitt, J.K. Luo, Y.Q. Fu, “ZnO based SAWand FBAR devices for bio-sensing applications,” J. Non-Newton. Fluid Mech, no 222, pp. 209-216, Feb. 2015.
[8] W. Pang, H.Y. Zhao, E.S. Kim, H. Zhang, H.Y. Yu, “Piezoelectric microelectromechanical resonant sensors for chemical and biological detection,” Lab Chip, no.12, pp. 29–44. 2012.
[9] L. Mai, J.Y. Lee, “Approach to improve ZnO-based FBAR devices,” Electronics Letters, vol. 43, no 13, pp. 735-737, Jun. 2007.
[10] W. Chen, “Research and modeling of thin film bulk acoustic wave filter FBAR,” Ph.D. dissertation, Dept. Elect. Eng. Zhejiang University, Hangzhou, 2005.
[11] S. J. Liu, “FBAR temperature sensor,” Ph.D. dissertation, Dept. Elect. Eng. Zhejiang University, Hangzhou, 2012.
[12] J Y Park, H C Lee, K H Lee, “Micromachined FBAR RF filters for advanced handset applications,” in IEEE International Conference on Transducers, Solid-state Sensors, Actuators & Microsystems, 2003, pp. 911-914.
[13] Q. X. Su, P. Kirby, E Komuro, et al. “Thin-film bulk acoustic resonators and filters using ZnO and Lead-Zirconium-Titanate thin film,” IEEE Transactions on Microwave Theory and Techniques, vol. 49, no. 4 pp. 769-778, Apr. 2001.
[14] A. Reinhardt, V. Laude, L. Robert, “Numerical simulation of FBAR’s,” in WCU 2003, Paris, 2003, pp. 1487-1494.

Xin Li received B.S., M.S. from Harbin Institute of Technology in 1997 and 1999, respectively and a Ph.D. degree in electronics science and technology from the Dalian university of technology in 2006. He is currently an associate Professor in Shenyang University of technology, China. He has published 10 papers in the areas of MEMS for RF wireless communications and wireless sensor.

Mengwei Liu received B.S., M.S., and Ph.D. degrees, all in electronics mechanical engineering from the Dalian University of Technology in 1999, 2002, and 2006, respectively. In Fall 2006, she joined the Institute of Acoustics, Chinese Academy of Science. She is an expert in piezoelectric and acoustic MEMS, have published more than 20 refereed papers and 3 issued patents in the field.

Yanlu Feng received B.S. and M.S. from the Shenyang University of Technology in 2013 and 2015, respectively. In Fall 2015, she joined microelectronics companies and engaged in MEMS research Work.